# Efficacy and connectivity of intracolumnar pairs of layer 2/3 pyramidal cells in the barrel cortex of juvenile rats

Dirk Feldmeyer[1,2], Joachim Lübke[2,3] and Bert Sakmann[1]

[1]*Abteilung Zellphysiologie, Max-Planck-Institut für medizinische Forschung, Jahnstr. 29, D-69120 Heidelberg, Germany*
[2]*Institut für Neurowissenschaften und Biophysik-Medizin, Forschungszentrum Jülich, D-52425 Jülich, Germany*
[3]*Institut für Anatomie und Zellbiologie der Albert-Ludwigs-Universität Freiburg, Albertstraße 17, D-79104 Freiburg i.Br, Germany*

**Synaptically coupled layer 2/3 (L2/3) pyramidal neurones located above the same layer 4 barrel ('barrel-related') were investigated using dual whole-cell voltage recordings in acute slices of rat somatosensory cortex. Recordings were followed by reconstructions of biocytin-filled neurones. The onset latency of unitary EPSPs was 1.1 ± 0.4 ms, the 20–80% rise time was 0.7 ± 0.2 ms, the average amplitude was 1.0 ± 0.7 mV and the decay time constant was 15.7 ± 4.5 ms. The coefficient of variation (C.V.) of unitary EPSP amplitudes decreased with increasing EPSP peak and was 0.33 ± 0.18. Bursts of APs in the presynaptic pyramidal cell resulted in EPSPs that, over a wide range of frequencies (5–100 Hz), displayed amplitude depression. Anatomically the barrel-related pyramidal cells in the lower half of layer 2/3 have a long apical dendrite with a small terminal tuft, while pyramidal cells in the upper half of layer 2/3 have shorter and often more 'irregularly' shaped apical dendrites that branch profusely in layer 1. The number of putative excitatory synaptic contacts established by the axonal collaterals of a L2/3 pyramidal cell with a postsynaptic pyramidal cell in the same column varied between 2 and 4, with an average of 2.8 ± 0.7 ($n = 8$ pairs). Synaptic contacts were established predominantly on the basal dendrites at a mean geometric distance of 91 ± 47 $\mu$m from the pyramidal cell soma. L2/3-to-L2/3 connections formed a blob-like innervation domain containing 2.8 mm of the presynaptic axon collaterals with a bouton density of 0.3 boutons per $\mu$m axon. Within the supragranular layers of its home column a single L2/3 pyramidal cell established about 900 boutons suggesting that 270 pyramidal cells in layer 2/3 are innervated by an individual pyramidal cell. In turn, a single pyramidal cell received synaptic inputs from 270 other L2/3 pyramidal cells. The innervation domain of L2/3-to-L2/3 connections superimposes almost exactly with that of L4-to-L2/3 connections. This suggests that synchronous feed-forward excitation of L2/3 pyramidal cells arriving from layer 4 could be potentially amplified in layer 2/3 by feedback excitation *within* a column and then relayed to the neighbouring columns.**

(Received 10 January 2006; accepted after revision 21 June 2006; first published online 22 June 2006)
**Corresponding author** D. Feldmeyer: Institut für Neurowissenschaften und Biophysik, AG Zelluläre Neurobiologie-Medizin, Forschungszentrum Jülich GmbH, Leo-Brandt-Straße, D-52425 Jülich, Germany.
Email: d.feldmeyer@fz-juelich.de

In the barrel cortex, as in other sensory cortices, excitation is relayed from the thalamus (in this case the ventral posterior medial nucleus, VPM) to layer 4 (L4) spiny neurones that are organized into clearly identifiable clusters of neurones termed barrels (Woolsey & van der Loos, 1970). The L4 spiny neurones in the barrel cortex are characterized by a vertical and largely column-restricted axonal arbour (Lübke *et al.* 2003). From layer 4, excitation spreads vertically to pyramidal cells in layer 2/3 (Laaris *et al.* 2000; Feldmeyer *et al.* 2002; Petersen *et al.* 2003) and in addition to those in layer 5A (Feldmeyer *et al.* 2005; Schubert *et al.* 2006). When synaptic depolarization of L2/3 pyramidal cells is suprathreshold, excitation spreads horizontally within layer 2/3 into the adjacent cortical columns and subsequently across the entire barrel field. *In vivo* whole cell recordings have suggested that most if not all L2/3 pyramidal cells respond with large EPSPs upon deflection of a single whisker having subthreshold receptive fields (RFs) that are broader than those of L4 spiny neurones (Brecht & Sakmann, 2002; Brecht *et al.* 2003). AP generation is sparse (Brecht *et al.* 2003) and suprathreshold receptive fields (RFs) are much broader for L2/3 pyramidal cells than for L4 spiny neurones (Simons, 1978, 1995; Armstrong-James & Fox, 1987;

 DOI: 10.1113/jphysiol.2006.105106

Armstrong-James *et al.* 1992; Armstrong-James, 1995; Moore & Nelson, 1998; Brecht & Sakmann, 2002; Brecht *et al.* 2003). The borders of the lateral spread of excitation within and across the barrel column corresponding to the stimulated whisker hair – the principal whisker (PW) column – over the cortical surface are predominantly determined by the spread of axonal arbours of L2/3 pyramidal cells in supragranular layers (Brecht *et al.* 2003; Petersen *et al.* 2003). The lateral borders of subthreshold receptive fields (PSP-RFs) or voltage-sensitive dye (VSD) images of L2/3 pyramidal cells are dynamic (Kleinfeld & Delaney, 1996; Laaris *et al.* 2000; Brecht *et al.* 2003; Petersen *et al.* 2003) depending on how many APs are generated in layer 2/3 of the PW column. However, contributions of L4 neurones to the RFs of L2/3 pyramidal cells may be of either intracortical (Armstrong-James *et al.* 1991; Fox *et al.* 2003) or subcortical (thalamic) origin (Simons & Carvell, 1989; Goldreich *et al.* 1999; Timofeeva *et al.* 2004; Kwegyir-Afful *et al.* 2005).

Previously we have characterized *in vivo* the properties of L4 and L2/3 neurones (Brecht & Sakmann, 2002; Brecht *et al.* 2003) and *in vitro* the synaptic connections between L4 and L2/3 neurones (Feldmeyer *et al.* 2002). To characterize possible anatomical and functional determinants of the dynamic borders of the cortical (whisker deflection) maps in layer 2/3 we have examined both efficacy and morphology of individual synaptic connections between 'barrel-related' (i.e. intracolumnar) L2/3 pyramidal cells. Specifically, we measured latency, time course, amplitude and amplitude variability of unitary EPSPs in paired recordings from L2/3 pyramidal cells. Furthermore, we determined the number of synaptic contacts and their dendritic location within the 'innervation domain' of L2/3 pyramidal cells.

The present functional and morphometric analysis of L2/3-to-L2/3 unitary connections is part of an effort to delineate the factors generating the wave of excitation streaming through the different layers of a cortical column when a single whisker is briefly deflected. In conjunction with the previously reported characterization of sub- and suprathreshold responses of L4 neurones *in vivo* and the sub- and suprathreshold responses of L2/3 neurones we can now provide estimates of the determinants of sparse AP coding of a sensory stimulus in the L2/3 network of a PW column.

## Methods

### Preparation

All experimental procedures were carried out according to the animal welfare guidelines of the Max-Planck Gesellschaft. Wistar rats (17–23 days old) were anaesthetized with halothane and decapitated, and slices of somatosensory cortex were cut in cold extracellular solution using a vibrating microslicer (DTK-1000, Dosaka Co. Ltd, Kyoto, Japan). In order to obtain slices in which connections along barrel rows were largely maintained, we used a modified version of the method described by Agmon & Connors (1991). The brain was removed from the skull and placed on a ramp with a 10 deg slope with the anterior face downhill. The midline was adjusted so that it was parallel to the walls of the ramp. Subsequently, a vertical cut at an angle of 45 deg to the midline was made. The tissue rostral to the cut was discarded and the brain was glued with the cut face downward onto the chilled stage of the slicer. Three to four ∼0.8–1.0 mm thick slices were cut and discarded. The remaining tissue was cut at slow speed and high vibration frequency into 300–400 $\mu$m thick 'semicoronal' slices each containing about one barrel row. Before recording, slices were incubated at room temperature (22–24°C) in an extracellular solution containing 1 mM $CaCl_2$ and 4 mM $MgCl_2$ to reduce overall synaptic activity and block NMDA receptors.

### Solutions

Slices were continuously superfused with an extracellular solution containing (mM): 125 NaCl, 2.5 KCl, 25 glucose, 25 $NaHCO_3$, 1.25 $NaH_2PO_4$, 2 $CaCl_2$ and 1 $MgCl_2$ bubbled with 95% $O_2$ and 5% $CO_2$. The pipette (intracellular) solution was based on K-gluconate and had a composition as follows: (mM) 105 K-gluconate, 30 KCl, 10 Hepes, 10 phosphocreatine, 4 ATP-Mg, 0.3 GTP (adjusted to pH 7.3 with KOH). The osmolarity of these solutions was 300 mosmol $l^{-1}$. Biocytin (Sigma, Munich, Germany) at a concentration of 3 mg $ml^{-1}$ was routinely added to the internal solution and cells were filled during 1–2 h of recording. For cell-attached stimulation (see below) we used a modified version of this solution containing (mM): 105 Na-gluconate, 30 NaCl, 10 Hepes, 10 phosphocreatine, 4 ATP-Mg, 0.3 GTP (adjusted to pH 7.3 with NaOH).

### Identification of synaptically connected neurones in the barrel cortex

Slices were placed in the recording chamber under an upright microscope (Nikon, Düsseldorf, Germany; fitted with ×4 plan/0.10 NA and ×60-W/1.20 objectives) with the pial surface pointing forward and the hippocampus to the left so that the L2/3 axons pointed into the slice. The barrel field was visualized at low magnification under bright-field illumination and can be identified in layer 4 as narrow dark stripes with evenly spaced, light 'hollows' (Agmon & Connors, 1991; Feldmeyer *et al.* 1999). Barrel structures were present in four to five slices but continuous rows of barrels (B, C, D rows) were visible only in two to three slices just above the fimbria-fornix and the lateral ventricle. Individual L2/3 pyramidal cells down to 170 $\mu$m depth in the slice were identified at ×60 magnification under infrared differential

interference contrast (IR-DIC) optics using a narrow bandwidth infrared filter to allow patching of neurones deep in the slice. This was necessary in order to obtain intact axonal arbours and simultaneously retain the barrel structure. After the electrophysiological recordings (see below) the slice was photographed at low power with the electrodes in place to obtain an image of the pre- and postsynaptic neurones and their location relative to the barrel structure in layer 4 (see online Supplemental material, Supplemental Fig. 1*A*–*C*).

### Electrophysiological recordings

Whole-cell voltage recordings from postsynaptic neurones were made using patch pipettes of ∼3.5–6 MΩ resistance pulled of thick borosilicate glass capillaries (outer diameter: 2.0 mm; inner diameter: 0.5 mm; F. Hilgenberg, Malsfeld, Germany). Searching for synaptic connections was performed in the loose seal configuration using a 'searching' patch pipette of ∼5–8 MΩ resistance (Feldmeyer *et al.* 1999). After establishing a loose seal (i.e. $R_{\mathrm{Seal}} < 1$ GΩ) on a potential presynaptic L2/3 pyramidal cell, the command potential was set to about −60 mV in current clamp mode. An AP was elicited by applying a 5 ms current pulse (0.2–2 nA). When an AP was elicited, this was in most cases visible as a small deflection on the voltage trace. In contrast to L4 spiny neurones, significantly higher stimulation intensities were necessary to evoke APs. When this loose-seal stimulation resulted in EPSPs in the postsynaptic L2/3 pyramidal cell at short latency (i.e. within 5 ms), the 'searching' pipette was withdrawn. The presynaptic cell was then re-patched with a new recording pipette (3.5–6 MΩ) filled with a biocytin-containing intracellular solution, and APs were elicited in the whole-cell (current clamp) mode. Occasionally cell-attached stimulation of the presynaptic neurone was also performed throughout the entire recording (rather than using the whole-cell configuration). In three cells where this was tested no difference in the recorded EPSP amplitude was found when the presynaptic neurone was stimulated initially in cell-attached and subsequently in whole-cell mode.

Somatic whole-cell recordings were performed at 34–36°C. Signals were amplified using an Axopatch 200B in combination with an Axoclamp 2B (Axon Instruments, Union City, CA, USA), for current clamp recordings filtered at 1–3 kHz and sampled at 2–10 kHz and for voltage clamp recordings filtered at 5 kHz and sampled at 10 kHz using the program 'Pulse' (v. 8.54, HEKA Elektronik, Lambrecht, Germany). Membrane potential fluctuations during current clamp recordings were ∼5 mV (peak to peak). Cell pairs in which a clear drift in the membrane potential was observed were omitted from the analysis. Acquired data were stored on the hard disk of a Macintosh computer for off-line analysis (Igor, Wavemetrics, Lake Oswego, OR, USA).

### Data analysis

EPSP amplitude, latency and kinetics were determined as previously described (Feldmeyer *et al.* 1999). In order to account for the extra-variance that resulted from membrane potential fluctuations, EPSP amplitudes were normalized to the mean membrane potential during the recording, assuming a linear current–voltage relationship and a near-zero reversal potential. This resulted in a slight reduction of the standard deviation of the EPSP amplitude and thus in a reduced coefficient of variation.

All recordings were inspected visually; failures were defined as events with amplitudes less than 1.5× the S.D. of the noise. In order to verify that small responses were not misclassified as failures due to a bad signal-to-noise ratio, failures were averaged in experiments with a high failure rate (> 10%, $n = 3$ out of 35). In all of these experiments the failure average was a flat line indicating that misclassification of records was negligible.

### Histological procedures

Following recording, slices were fixed at 4°C for at least 24 h in 100 mM phosphate-buffered saline (PBS, pH 7.4), containing either 4% paraformaldehyde or 1% paraformaldehyde and 2.5% glutaraldehyde. Slices containing biocytin-filled neurones were processed using a modified protocol previously described (Lübke *et al.* 2000). For light microscopy they were incubated overnight in PBS–avidin-biotinylated horseradish peroxidase (ABC-Elite, Camon, Wiesbaden, Germany) containing 0.1% Triton X-100. Slices were then reacted using 3,3-diaminobenzidine (DAB) as a chromogen under light microscopic control until dendritic and axonal arborizations were clearly visible. Slices were then briefly postfixed in 0.1% $OsO_4$ (1–3 min). After several rinses in 100 mM PBS they were mounted on slides, embedded in Moviol (Hoechst AG, Frankfurt, Germany) and enclosed with a coverslip. For electron microscopy, slices were cryo-protected in PBS-buffered sucrose, freeze–thawed in liquid nitrogen and then incubated overnight in the ABC solution at 4°C. After the DAB reaction they were post-fixed in 0.5% $OsO_4$ (30–45 min), then dehydrated through an ascending series of ethanol and finally flat-embedded in epoxy resin (Durcopan, Fluka AG, Germany) using a standard electron microscopic embedding protocol. Electron microscopy (EM) was carried out on one pair to confirm putative light microscopically identified synaptic contacts (Feldmeyer *et al.* 2002). Serial ultrathin sections through the dendritic and axonal domain were cut with an ultramicrotome (Leitz UItracut, Hamburg, Germany)

and analysed for synaptic contacts using a Zeiss EM 10 electron microscope (Zeiss, Oberkochen, Germany).

### Morphological reconstructions of biocytin-filled synaptically coupled neurones

Biocytin-labelled pairs of neurones were examined under the light microscope at high magnification to identify putative synaptic contacts. Representative pairs were photographed at low magnification to document dendritic and axonal arborization; potential synaptic contacts were identified as close appositions of a synaptic bouton and the postsynaptic dendrite in the same focal plane at a final magnification of ×1200 (×100 objective and ×12 eyepiece; Fig. 4). Subsequently, biocytin-labelled pairs of neurones were reconstructed with the Neurolucida software (MicroBrightfield, Colchester, VT, USA) using an Olympus BX50 microscope (Olympus, Hamburg, Germany) at a final magnification of ×780 to ×1200. During the reconstruction bouton counts were made on both deep and superficial axonal collaterals in order to determine their bouton density; the total axonal length of a neurone as well as its length within a barrel column was measured using Neuroexplorer software (MicroBrightfield, Colchester VT, USA). Furthermore, these reconstructions provided the basis for the quantitative morphological analysis of the location of the somata within the slice and the number and the dendritic location of putative synaptic contacts. For all data, means ± S.D. are given. In addition, the length of the apical dendrite, the apical tuft (defined as the part of the apical tuft following the bifurcation of the first-order apical dendrite) and the number of nodes in the apical tuft were determined. Data were not corrected for shrinkage.

### Axonal and dendritic density maps

Two-dimensional (2D) maps of axonal and dendritic 'length density' were constructed using the computerized 3D reconstructions (for details see Lübke *et al.* 2003). The length of all axonal and dendritic branches was projected in the 2D plane and measured in a 50 $\mu$m × 50 $\mu$m Cartesian grid, yielding a raw density map. For alignment of these maps with respect to the barrel centre, barrel borders were identified in the low power (× 4 objective) bright-field micrographs made from the acute brain slice (Lübke *et al.* 2000, 2003; Feldmeyer *et al.* 2002). Spatial low-pass filtering of these maps was performed by 2D convolution with a Gaussian kernel ($\sigma = 50\,\mu$m) and continuous 2D density functions were constructed using bicubic interpolation in Mathematica 4.1 (Wolfram Research, Champaign, IL, USA). The axonal and the dendritic 'length density' maps thus obtained were then multiplied in order to calculate the predicted 'innervation domain' between pairs of L2/3 pyramidal cells (Lübke *et al.* 2003).

## Results

Dual whole-cell recordings from synaptically coupled pyramidal cells ($n = 36$) were established in the region of layer 2/3 located directly above the barrels in layer 4 of the somatosensory cortex. L2/3 pyramidal cells had a mean resting potential of $-76 \pm 4$ mV, and their regular AP firing (with firing threshold of about $-35$ mV) upon injection of 500 ms current pulses allowed an unambiguous identification as pyramidal cells; this was subsequently confirmed by histochemical processing. Before obtaining a synaptically connected pair of neurones, between 1 and 30 cells had to be tested. As for L4-to-L4 pairs and L4-to-L2/3 pairs (Feldmeyer *et al.* 1999, 2002) there appeared to be clusters of L2/3 pyramidal cells within which the connectivity was particularly high; however, this was not quantified. The distance between the somata of synaptically coupled L2/3 pyramidal cells ranged from 10 to 89 $\mu$m (average $42 \pm 20\,\mu$m), i.e. virtually all of the pyramidal cell pairs investigated here were located within the same barrel column. L2/3 pyramidal cells from which recordings were obtained were located between 40 and 176 $\mu$m deep in the slice (average $110 \pm 23\,\mu$m), $224 \pm 74\,\mu$m from the layer 4 border and $286 \pm 78\,\mu$m from the pia. Quantitative morphological analysis was performed only for those L2/3 pyramidal cell pairs that, after histochemical processing, showed good staining of both the dendritic and axonal arbours.

### Functional properties of synapses between L2/3 pyramidal cell pairs

To characterize the connections between L2/3 pyramidal cells functionally, unitary EPSPs in pyramidal cells were analysed by measuring their latency, rise time, peak amplitude and decay time course in detail. Unitary EPSPs were elicited at a frequency of 0.033–0.05 Hz (every 20–30 s). Higher stimulation frequencies resulted in a rapid decrease in the unitary EPSP amplitude. However, when returning to lower stimulation rates, the EPSP amplitude recovered.

As for synaptically coupled pairs between L4 spiny neurones and L2/3 pyramidal cells (and in contrast to pairs between spiny neurones in layer 4; Feldmeyer *et al.* 1999), pairs between layer 2/3 pyramidal cells showed a relatively low spontaneous synaptic activity (Feldmeyer *et al.* 2002) which facilitated the analysis of EPSPs and the detection of small EPSPs.

**EPSP latency and time course.** Figure 1*A* shows a presynaptic AP and an evoked unitary EPSP in a pre- and postsynaptic L2/3 pyramidal cell, respectively. The latency between the peak of the AP and the unitary EPSP at an individual L2/3–L2/3 synaptic connection showed little variation (at most twofold) and latency histograms were

narrow and showed a single peak (Fig. 1*B*). They are thus similar to the connection between L4 spiny neurones and L2/3 pyramidal cells (Feldmeyer *et al.* 2002). The data shown in Fig. 1*C* indicate that the average latency of EPSPs at synapses between L2/3 pyramidal cells ranged from 0.6 to 1.9 ms for individual connections and was on average $1.1 \pm 0.4$ ($n = 21$; temperature 35–37°C), indicating that the postsynaptic neurone is rapidly recruited.

The EPSP rise time (20–80% of the peak amplitude) was on average $0.7 \pm 0.2$ ms ($n = 35$), and the decay

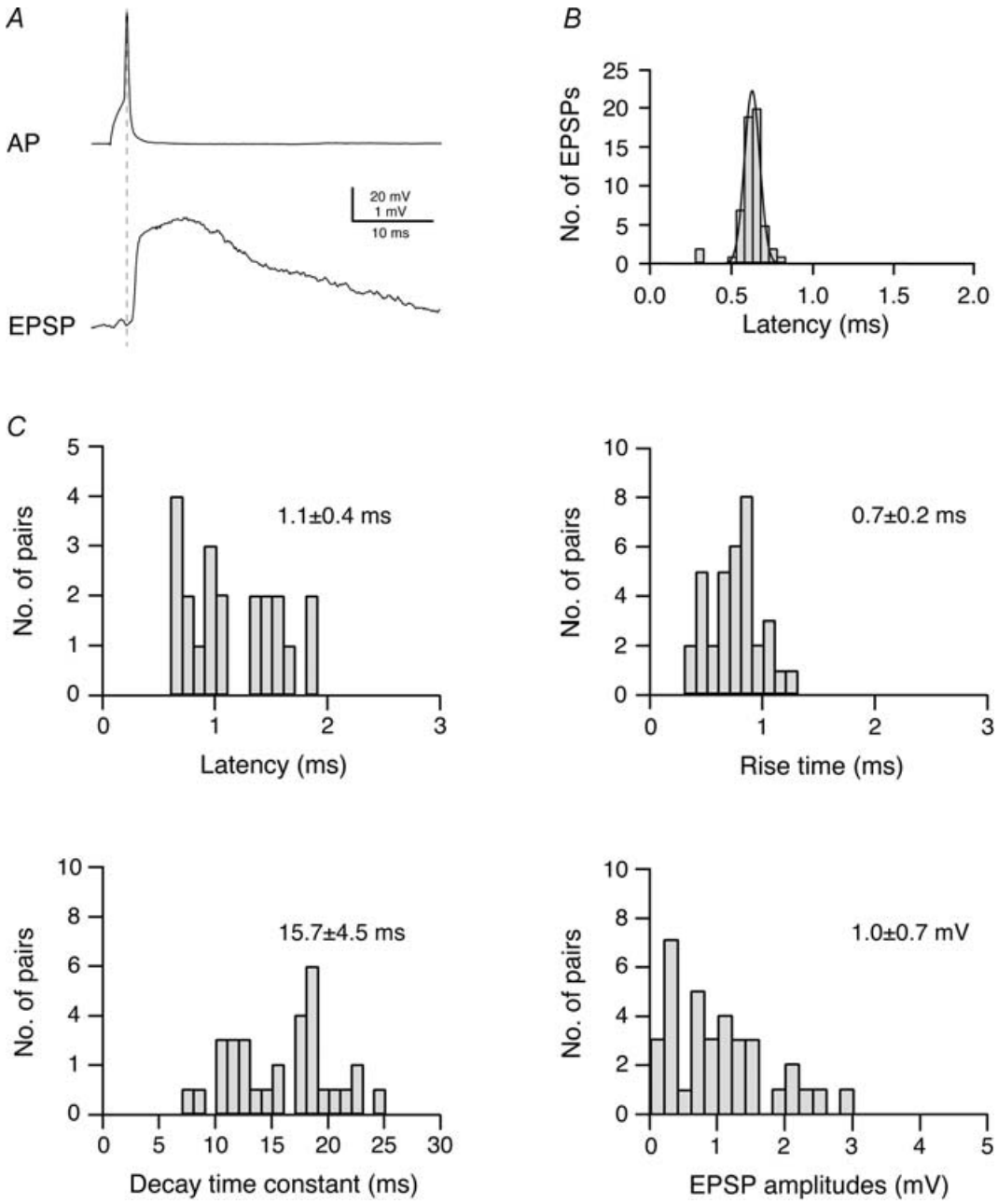


**Figure 1. Time course and amplitude of EPSPs in L2/3 pyramidal cells of the barrel cortex**
*A*, original recording of a presynaptic AP and a postsynaptic EPSP in a synaptically coupled pair of L2/3 pyramidal cells. *B*, distribution of EPSP latencies in an individual synaptically connected pair of L2/3 pyramidal cells; the continuous curve is a single Gaussian fit. Note that the latency distribution for this connection is narrow. *C*, distributions of EPSP latencies, 20–80% rise times, decay time constants and EPSP amplitudes for L2/3 pyramidal cell connections. Latencies were calculated as the time between the peak of the AP and the onset of the EPSP (indicated by the dashed line in *A*) and the onset of the EPSP. Decay times were obtained by fitting a single exponential to the falling phase of the EPSP.

time constant was $15.7 \pm 4.5$ ms ($n = 33$). The EPSP amplitude for the L2/3-to-L2/3 pyramidal cell connection was on average $1.0 \pm 0.7$ mV (range 0.08–2.9 mV; $n = 35$; Fig. 1*C*). Within a barrel column there was no correlation between the EPSP amplitude and the distance between the pre- and postsynaptic L2/3 pyramidal cell bodies.

Voltage clamp recordings from synaptically coupled L2/3 pyramidal cells were performed to study the properties of the synaptic currents that mediated the EPSPs at the L2/3-L2/3 pyramidal cell synapse. When using 70–80% series resistance compensation, mean EPSC amplitudes varying from 6 to 111 pA were recorded; the average between pairs was $58 \pm 35$ pA ($n = 7$). The mean EPSC rise time was $0.35 \pm 0.16$ ms and the mean decay time constant $3.7 \pm 1.2$ ms (see Supplemental Online Material, Supplemental Fig. 3).

As for other synaptic connections (e.g. Feldmeyer *et al.* 2002), the decay time constant of the EPSP was significantly longer than that of the EPSC measured at the soma in the same neurone (18.3 ms *versus* 3.7 ms; $P < 0.001$). The EPSP time course is likely to be shaped to a considerable degree by the membrane time constant of the postsynaptic L2/3 pyramidal cell (which is $10.9 \pm 2.4$ ms; $n = 35$). The EPSP decay time constant was significantly longer ($P < 0.0001$) than the membrane time constant. Therefore, dendritic filtering may contribute to its slow time course.

**Reliability of synaptic transmission.** Intralaminar synaptic transmission between pairs of L2/3 pyramidal cells is reliable (Fig. 2) as observed for other intracortical connections (Stratford *et al.* 1996; Feldmeyer *et al.* 1999,

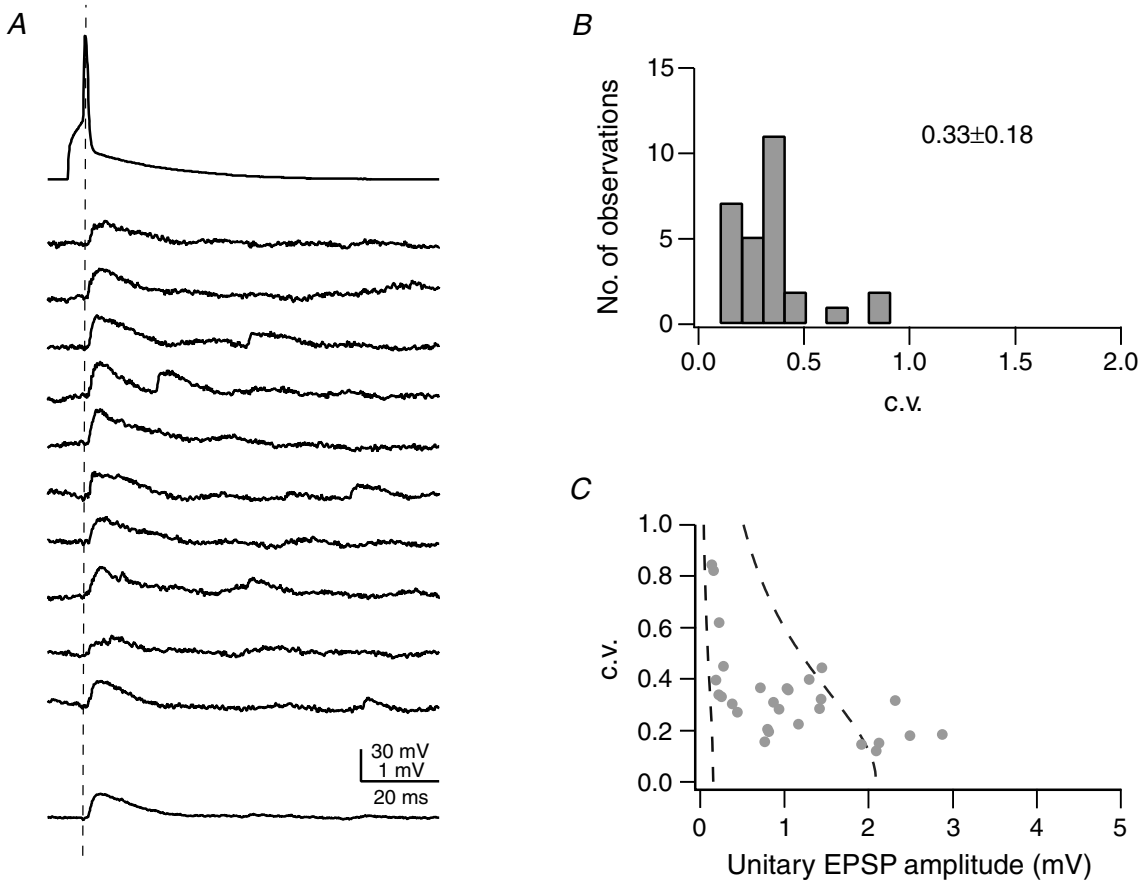


**Figure 2. Reliability of synaptic connections between pairs of L2/3 pyramidal cells**
*A*, examples of 10 successive unitary EPSPs in response to a presynaptic AP (top trace); the bottom trace represents the average EPSP waveform. The dashed line indicates the peak of the AP. *B*, distribution of the c.v. of unitary EPSP amplitudes calculated in 28 L2/3-to-L2/3 connections from 50–200 trials (stimulation frequency 0.05–0.1 $s^{-1}$); the average c.v. was $0.33 \pm 0.18$. *C*, relationship of c.v. and EPSP peak amplitude in the postsynaptic L2/3 pyramidal cell. The two dashed lines in *C* represent the predictions of single binomial release statistics for the c.v. as a function of EPSP amplitude assuming three synaptic contacts (close to the average number of contacts, Table 1), and $q_S = 0.05$ mV (right curve) and $q_S = 0.7$ mV (left curve); $p_r$ increases from 0.08 to 0.6 (right curve) and from 0.05 to 1.0 (left curve). The $p_r$ values refer to the two endpoints of each curve. Connections with large mean EPSP amplitudes are not well described by binomial release statistics.

2002). Seventy-five per cent of the connections ($n = 21$ out of 28 analysed) showed virtually no failures (i.e. less than 2%) and only in four pairs was the percentage of failures higher than 10%. On average, the failure rate of the L2/3–L2/3 connections was $3.2 \pm 7.8$%.

In 28 synaptically coupled cell pairs, the coefficient of variation (c.v.) of unitary EPSPs ranged from 0.11 to 0.84, with a mean of $0.33 \pm 0.18$ (Fig. 2*B* and *C*), again suggesting a high reliability of these connections.

As described for layer 5B pyramidal cell pairs (Markram *et al.* 1997), for L4 spiny neurone pairs and for L4-to-L2/3 pairs (Feldmeyer *et al.* 1999, 2002), the c.v. was inversely related to the amplitude of the unitary EPSP. In simple binomial models of synaptic transmission this is to be expected when the unitary EPSP amplitude is primarily determined by the release probability ($p_r$). For the L2/3–L2/3 connection, binomial release with varying quantal content but similar release probabilities have recently been demonstrated by Koester & Johnston (2005).

Calculations of limiting curves assuming binomial release with $\text{c.v.} = \sqrt{[(1 - p_r)/(n_b p_r)]}$ and $p_r = \Delta V/(n_b q_s)$, and fixed values for the number of release sites ($n_b$) and the quantal amplitude ($q_S$) were not entirely satisfactory, since EPSP amplitudes larger than 2.0 mV were not included. To obtain limits for $n_b$ and $q_S$, we assumed that $n_b$ was 3 (i.e. close to the mean number of putative synaptic contacts as determined by light microscopical examination). The two limiting curves in Fig. 2*C* were calculated for $q_S = 0.05$ and 0.70 mV. The range of quantal EPSP amplitudes is smaller for intralaminar connection between L2/3 pyramidal cells than for the L4-to-L4 and L5-to-L5 connections in layer 5B (Markram *et al.* 1997; Feldmeyer *et al.* 1999; Feldmeyer & Sakmann, 2000) but larger than that observed for the interlaminar L4-to-L2/3 connection (Feldmeyer *et al.* 2002).

**Paired pulse behaviour and EPSP summation.** To test the frequency dependence of synaptic transmission between pairs of synaptically connected L2/3 pyramidal cells, we recorded bursts of five unitary EPSPs at various frequencies (corresponding to interstimulus intervals of 10, 20, 50, 100, 200 ms; $n = 5$). Figure 3*A* shows that EPSP trains in a L2/3 pyramidal cell depressed at most burst frequencies tested. Interestingly, facilitation occurred occasionally at higher burst frequencies. The EPSP amplitude ratio (i.e. the ratio of the 2nd, 3rd, 4th and 5th EPSP relative to the 1st EPSP) is plotted in Fig. 3*B*. For the 2nd EPSP the depression was already $0.61 \pm 0.41$ and $0.73 \pm 0.23$ for the 10 ms and 50 ms interstimulus interval) and became progressively larger for successive EPSPs in the train, being particularly strong for the 5th EPSP in the train ($0.23 \pm 0.04$ and $0.55 \pm 0.20$ for the 10 ms and 50 ms interstimulus interval).

## Dendritic and axonal morphology of synaptically coupled L2/3 pyramidal cells

Of the synaptically coupled pairs of L2/3 pyramidal cells, 11 (i.e. 22 neurones) were selected for further quantitative morphological analysis. About one-third of these neurones

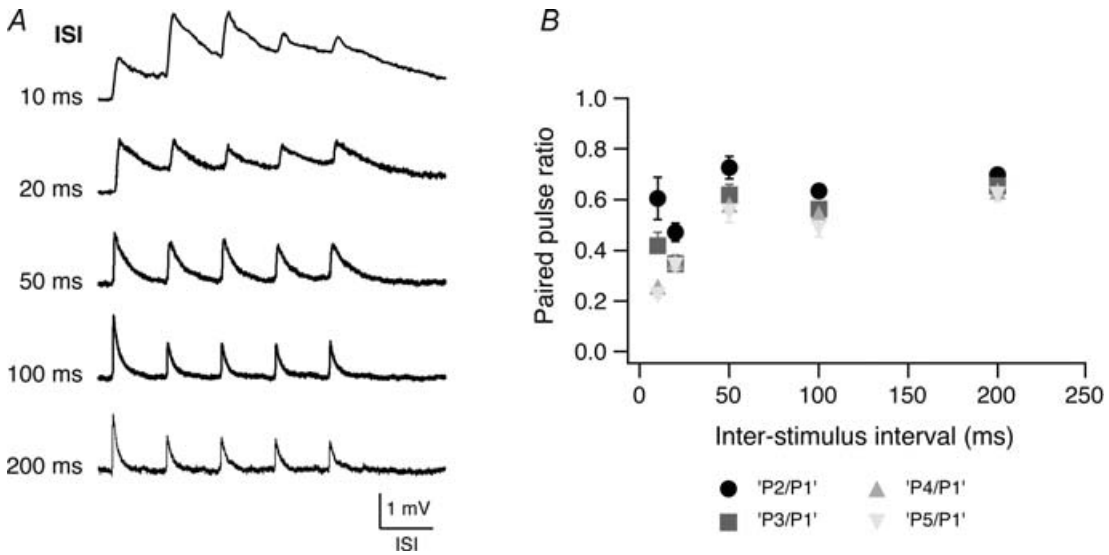


**Figure 3. Paired pulse ratio in pairs of L2/3 pyramidal cell**
*A*, train of five consecutive EPSPs at different interstimulus intervals as indicated on the left. At most connections EPSP amplitude depression occurred at all frequencies tested while summation of EPSPs was apparent only at an interstimulus interval of 10–20 ms. The horizontal scale bar corresponds to the interstimulus time of each train. *B*, amplitude ratios (●, 2 EPSP/1 EPSP; grey square, 3 EPSP/1 EPSP; grey triangle, 4 EPSP/1 EPSP, grey inverted triangle, 5 EPSP/1 EPSP) plotted as a function of the interstimulus interval. For short interstimulus intervals (10 ms and 20 ms), the baseline to determine the EPSP amplitudes in the train was obtained by linear extrapolation of the decay phase of the preceding EPSP.

($n = 8$) were in the lower half of layer 2/3 while the rest ($n = 14$) were located in the upper half of layer 2/3. A clear correlation between apical dendritic length of L2/3 pyramidal cells, the length of dendritic collaterals in the apical tuft and the number of nodes in the tuft was revealed using a Spearman rank order test, with correlation coefficient ($r_s$) of 0.708 and 0.765, respectively. Pyramidal cells in the lower half of layer 2/3 have long apical dendrites (up to 440 $\mu$m long; mean $278 \pm 89$ $\mu$m) before bifurcating close to layer 1 and forming only comparatively small apical tufts with a dendritic length of $1033 \pm 552$ $\mu$m and $7.0 \pm 4.1$ bifurcating nodes (Fig. 5*A*, Neurolucida reconstruction). In contrast, pyramidal cells in the upper half of layer 2/3 display a relatively short apical dendrite (10–140 $\mu$m; average $79.8 \pm 39.1$ $\mu$m) that bifurcates in a terminal tuft with a significantly longer dendritic length of $1863 \pm 628$ $\mu$m ($P = 0.002$, unpaired, two-tailed $t$ test) and significantly more bifurcating nodes ($17.2 \pm 7.4$; $P = 0.0005$, unpaired, two-tailed $t$ test) (Fig. 4*A*, halftone image; Fig. 5*B*, Neurolucida reconstruction). In addition, the axonal collaterals of the former pyramidal cells appear to ascend to the upper portion of layer 2/3, in contrast to the more horizontal collaterals formed by the more superficial pyramidal cells (Fig. 5; cf. Lübke *et al.* 2003). The total axonal length and that within the supragranular layer were statistically different for deep

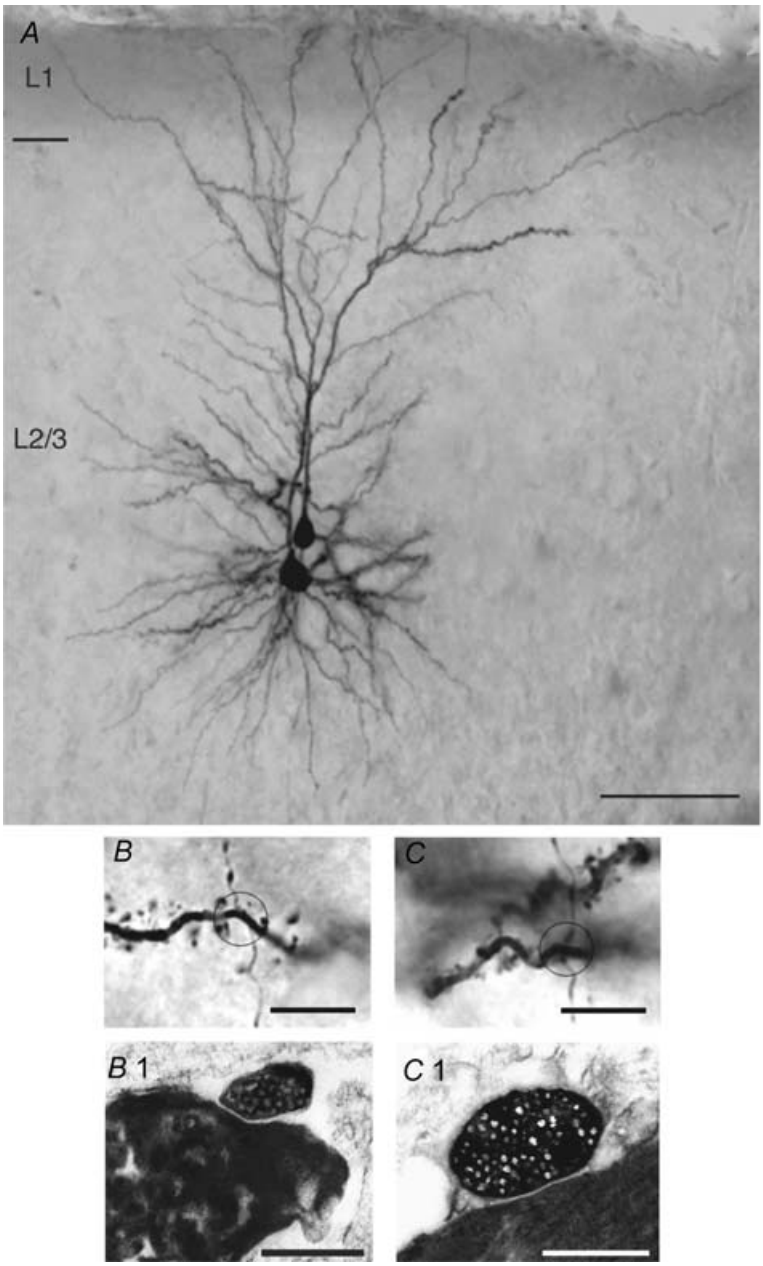


**Figure 4. Half-tone image of a pair of synaptically coupled L2/3 pyramidal cells including the light and electron microscopic identification of synaptic contacts**
*A*, low magnification light microscopic image of two synaptically coupled pyramidal cells filled with biocytin. Both pyramidal cells were located in the middle portion of layer 2/3. Note the elaborate symmetric basal dendritic field and the apical dendrites forming extensive tufts terminating in layer 1. Calibration bar, 100 $\mu$m. *B* and *C*, high magnification of the synaptic contacts established by *en passant* axonal collaterals of the presynaptic neurone on different basal dendrites of the postsynaptic L2/3 pyramidal cells. The calibration bar is 5.0 $\mu$m for both panels. *B1* and *C1*, both light microscopically identified synaptic contacts were identified at the electron microscopic level. The synaptic boutons of the presynaptic axon collaterals are clearly identifiable by their content of transmitter vesicles. The calibration bar is 1.0 $\mu$m for both panels.

and superficial pyramidal cells, with $22095 \pm 4884\ \mu$m ($n = 10$ pyramidal cells) *versus* $12931 \pm 2857\ \mu$m ($n = 4$; $P = 0.026$) and $12226 \pm 3336\ \mu$m *versus* $6911 \pm 2772\ \mu$m, respectively ($P = 0.039$); however, their axonal length within a barrel column did not differ significantly (total length: $11329 \pm 2585\ \mu$m *versus* $7823 \pm 1811\ \mu$m; $6414 \pm 1715\ \mu$m *versus* $4164 \pm 1183\ \mu$m; $P > 0.05$).

**Number and location of synaptic contacts.** Figure 4*A* is a photomontage showing a pair of synaptically coupled L2/3 pyramidal cells that were filled with biocytin during recording. Two synaptic contacts were identified following light microscopic examination as close appositions of postsynaptic dendrites and presynaptic axon as can be seen in Fig. 4*B* and *C*. Subsequent serial EM analysis through the dendritic segments was performed to confirm that these two potential contacts were indeed synaptic contacts. Figure 4*B1* and *C1* shows synaptic boutons of the presynaptic L2/3 pyramidal cell axon, clearly identifiable by their neurotransmitter vesicles, which are in close apposition to dendritic structures of the postsynaptic L2/3 pyramidal cell. In this particular example, both synaptic contacts were established directly on dendritic shafts (Fig. 4*B1* and *C1*). However, about two-thirds of synaptic contacts are on dendritic spines as revealed by analysis of axon targets for five single L2/3 pyramidal cells (Supplemental Online Material; Supplemental Fig. 4).

The dendritic location and distance of synaptic contacts from the soma were measured from the Neurolucida reconstructions of dendritic and axonal profiles. The insets in Fig. 5*A* and *B* illustrate the location of the three light microscopically identified synaptic contacts, identified for both pairs of neurones at the light microscopic level. Only the dendritic configuration of the target cell (white) is illustrated together with the location of the putative synaptic contacts (light blue squares). In the two cell pairs shown here all synaptic contacts were found exclusively on second- to fourth-order basal dendrites.

For eight reconstructed L2/3 pyramidal cell pairs, the mean number of synaptic contacts was $2.8 \pm 0.7$ with a minimum of two and a maximum of four (Fig. 6*A*, inset). Synaptic contacts were located between 18 and 170 $\mu$m from the soma with an average distance of $91 \pm 47\ \mu$m (Fig. 6*A*). The vast majority (95%) was located on basal dendrites; only a small fraction (5%) was located on apical oblique dendrites; no synaptic contacts were found in the terminal tuft dendrites (see Table 1).

As there is little variation in both EPSP amplitude and the number of synaptic contacts, it is not possible to judge whether a correlation exists between the number of synaptic contacts per connection and the mean EPSP amplitude (Fig. 6*B*). Similar to L5–L5 and L4–L2/3 pairs (but contrary to the finding for L4–L4 pairs), there was no negative correlation between EPSP amplitude and the geometric distance of synaptic contacts from the soma (Fig. 6*C*). The large differences in the mean amplitude of unitary EPSPs between different L2/3 pyramidal cell pairs may therefore be determined to a significant degree by differences in the functional properties of the projection and the target neuron (Koester & Johnston, 2005), rather than by differences in their morphology, as has been suggested previously for connections between L5B pyramidal cells (Markram *et al.* 1997). Furthermore, no correlation was found between EPSP decay time constant and the average distance of synaptic contacts in L2/3–L2/3 pyramidal cell pairs (data not shown).

## Axonal 'projection' fields, dendritic 'reception' fields and synapse locations

**Overlap of 'projection' and 'reception' fields in the L2/3-to-L2/3 pyramidal cell pairs.** When all reconstructions of L2/3 pyramidal cell pairs (without obvious truncations in the axonal arbour down to layer 5; $n = 8$) are superimposed and aligned with respect to the barrel centre (Fig 7*A* and *B*) it is clearly evident that within a barrel column the 'projection' field of a presynaptic L2/3 axon overlaps to a very large extent with the dendritic 'reception' field of the postsynaptic L2/3 pyramidal cell. To quantify this overlap the axonal length of the presynaptic pyramidal cell axon was measured using a $50\ \mu\text{m} \times 50\ \mu$m grid superimposed on 2D projections of 3D reconstructions of the cell pairs (see Lübke *et al.* 2003). We then constructed a 2D map of the axonal 'length density' of L2/3 axons using bicubic interpolation of the original grid points yielding an 'average' axonal projection of the presynaptic L2/3 pyramidal cells. The reference point for alignment of the reconstructions was either the centre of the barrel (Fig. 7*C1*), or the soma of the postsynaptic L2/3 pyramidal cell (Fig. 7*D1*). The map of the L2/3 axonal 'length density' clearly shows that the axon of the presynaptic L2/3 pyramidal cell projects widely into neighbouring barrel columns (Fig. 7*C1* and *D1*) as was reported in previous *in vitro* and *in vivo* studies (Gottlieb & Keller, 1997; Brecht *et al.* 2003). Comparing the outline of the average barrel column to the contour line including 80% of the presynaptic L2/3 axonal 'length density' shows that its density map includes at least the two neighbouring barrel columns (i.e. at least one on each side) both within layer 2/3 as well as in layers 5 and 6. In layer 2/3 the width of the 2D map is somewhat larger than in layers 5 and 6 (cf. Fig. 7*C1* and *D1*; Table 2). In contrast, there is virtually no lateral projection of the L2/3 pyramidal cell axonal domain in layer 4 (cf. Lübke *et al.* 2003). In supragranular layers the total axonal length of a single pyramidal cell is on average $8715 \pm 3638\ \mu$m of which $4704 \pm 1924\ \mu$m is within the barrel column (cf. Fig. 8*A* and *B*). However, the total axonal length in particular that outside the 'home' barrel column is likely to be underestimated.

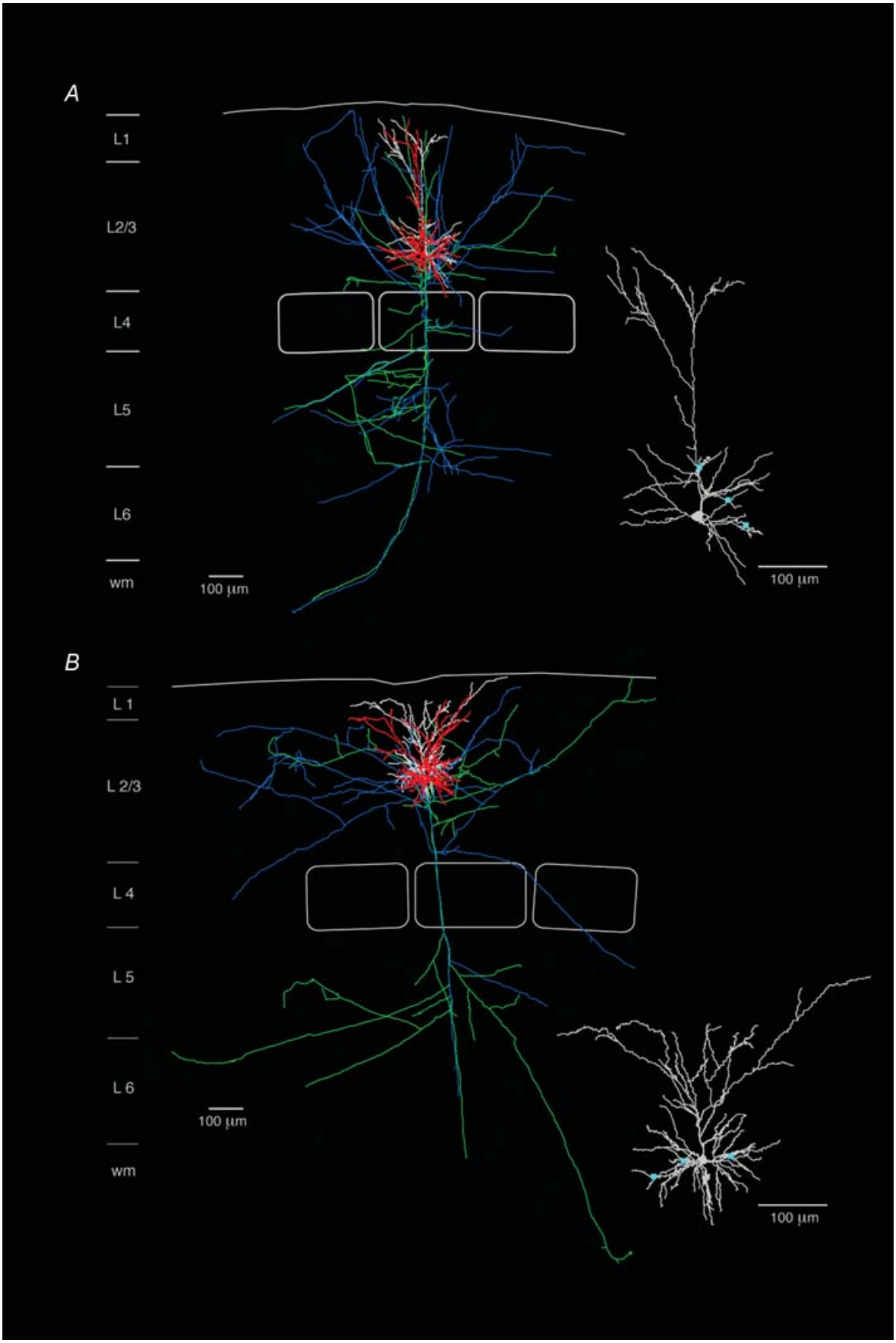

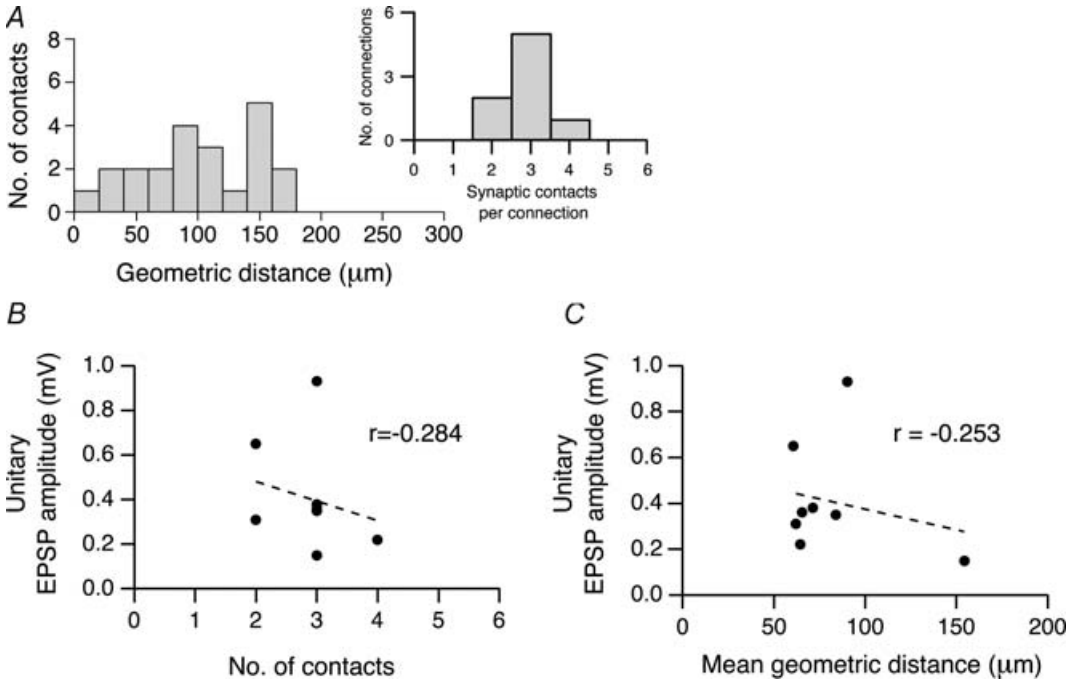


**Figure 6. Number and location of synaptic contacts on dendrites**
*A*, histogram showing the geometric distances of light microscopically identified synaptic contacts from the soma in eight L2/3 pyramidal cell pairs ($n = 22$ contacts). Inset, distribution of the number of synaptic contacts per individual connection. *B*, relationship between the unitary EPSP amplitude in the postsynaptic L2/3 pyramidal cells and the number of synaptic contacts per connection. The correlation coefficient *r* obtained for *B* was –0.284. *C*, relationship between the unitary EPSP amplitude and the mean geometric distance from the soma of synaptic contacts in a connection. The correlation coefficient *r* was – 0.253. For both graphs, the correlation was statistically not significant.

Figure 7*C2* illustrates the 'dendritic density' maps of the postsynaptic L2/3 pyramidal cells. Here, all reconstructed pairs were also aligned with respect to the centre of the 'home' barrel. The contour line including 80% of all postsynaptic L2/3 dendritic length lies within the borders of the barrel column. Figure 7*D2* shows the dendritic density map, when normalized to the postsynaptic pyramidal cell somata which is much more localized than the barrel-centred map.

**Innervation domain and location of synaptic contacts.** We then calculated the predicted innervation domain by multiplying the axonal 'length density' and the dendritic 'length density' assuming that synaptic connections between axons and dendrites in a given region are formed by a random encounter (Fig. 7*C3* and *D3*). The outline of this predicted innervation domain is limited by the extent of the dendritic arborization of the postsynaptic neurone. The sharp delineation of this innervation domain of L2/3 pyramidal cells is particularly clear when presynaptic axonal and postsynaptic dendritic length maps are normalized with respect to the somata of the postsynaptic L2/3 pyramidal cells. The 2D projected dimensions of the innervation domain are about 233 $\mu$m (horizontal) and 264 $\mu$m (vertical; see Table 2). The axonal arbours of the presynaptic L2/3 pyramidal cells

**Figure 5. Reconstructions of two pairs of synaptically coupled L2/3 pyramidal cells**
Neurolucida reconstructions of two pairs of synaptically coupled L2/3 pyramidal cells, located in the lower (*A*) and upper half (*B*) of layer 2/3, respectively. For both pairs of neurones, the dendritic configuration of the presynaptic L2/3 pyramidal cell is drawn in red with its axon in blue and the postsynaptic L2/3 pyramidal cell is drawn in white with its axon in green. Scale bar, 100 $\mu$m. Pyramidal cells in the lower half of layer 2/3 display a more prominent apical dendrite with a number of oblique collaterals, extending up to 300 $\mu$m before bifurcating close to layer 1 giving rise to a terminal tuft. In contrast, pyramidal cells in the upper half of layer 2/3 have only a short apical trunk that bifurcates after ~30–150 $\mu$m into an extensive terminal tuft (Fig. 5*B*). The insets in panels *A* and *B* show the location of synaptic contacts (blue squares) on the postsynaptic neurone. Note that most synaptic contacts are found on basal dendrites.

**Table 1. Number and distribution of synaptic contacts established by axonal collaterals of presynaptic L2/3 pyramidal cells with postsynaptic L2/3 pyramidal cell dendrites.**

| | Occurrence (in % of total) | Number of synaptic contacts |
|---|---|---|
| 1° Basal | 4.5 | 1 |
| 2° Basal | 27.3 | 6 |
| 3° Basal | 40.9 | 9 |
| 4° Basal | 22.7 | 5 |
| 1° Apical oblique | 0.0 | 0 |
| 2° Apical oblique | 0.0 | 0 |
| 3° Apical oblique | 4.5 | 1 |

Ten unidirectional barrel-related L2/3-L2/3 connections were analysed. The number of putative light-microscopically identified synaptic contacts was 22. '°' refers to the order of a dendritic branch. Basal 1° would be a dendrite arising from the soma, apical oblique 1° would be a dendrite arising from the main apical trunk.

**Table 2. Dimensions of 2D maps of L2/3 pyramidal cell dendrite and axon density.**

| Structure | Barrel-centred ($\mu$m) | Postsynaptic map soma-centred map ($\mu$m) |
|---|---|---|
| Axon arbour of presynaptic L2/3 pyramidal cell | | |
| Height | 1273 | 1314 |
| Width in layer 2/3 | 966 | 831 |
| Width in layer 4 | 458 | 368 |
| Width in layer 5 | 764 | 627 |
| Dendrites of postsynaptic L2/3 pyramidal cell | | |
| Height | 495 | 440 |
| Width | 429 | 270 |
| Innervation domain | | |
| Height | 366 | 264 |
| Width | 354 | 233 |
| Average barrel and layer 2/3 dimensions | | |
| Barrel height | $201 \pm 26$ | |
| Barrel width | $322 \pm 29$ | |
| Layer 2/3 height | $432 \pm 80$ | |

2D axonal and dendritic 'length density' maps were generated from reconstructions of eight unidirectional synaptic connections (see Methods). Dimensions refer to the maximal vertical or horizontal distance (for layers 2/3 and 5) between the contour line including 80% of all axonal or dendritic length. Horizontal dimensions in layer 4 were determined at the barrel centre.

predominantly overlap with the basal dendritic field of the postsynaptic neurones (Fig. 7*C3* and *D3*). Within this round to oval innervation domain, the L2/3 axonal length was 2881 $\mu$m (barrel-centred); with a bouton density of $0.30 \pm 0.02\ \mu\text{m}^{-1}$, this corresponds to roughly 900 synaptic boutons per pyramidal cell in the innervation domain. In the barrel-centred map, the L2/3 dendritic length was ~3200 $\mu$m, i.e. the ratio of dendritic to axonal length was 1.11. With these values and a spine density on the basal dendrites of $0.97 \pm 0.07\ \mu\text{m}^{-1}$ (Lübke *et al.* 2003), the fraction of synaptic contacts established by the axonal collaterals of the intracolumnar presynaptic L2/3 pyramidal cells can be estimated (see below).

To estimate whether the extent of the innervation domain of the presynaptic L2/3 pyramidal cell axonal collaterals and postsynaptic L2/3 pyramidal cell dendrites corresponds to the actual density of innervation, the location of synaptic contacts was marked in the innervation domain (Fig. 9; light blue dots). Indeed, the majority of synaptic contacts were located within the borders of the innervation domain. This is the case irrespective of whether the reconstructions were centred with respect to barrels (Fig. 9*A*) or to L2/3 pyramidal cell somata (Fig. 9*B*). Only 2 or 0 of 22 contacts (9 or 0%, barrel- or soma-centred maps, respectively; $n = 8$ L2/3 pyramidal cell pairs) were located outside the predicted innervation domain.

## Discussion

The L2/3 pyramidal cells, which anatomically and functionally can be classified as 'barrel-related' pyramidal cells and whose mutual synaptic connections we investigated here, are part of an excitatory network in their home (PW) barrel column. Synaptic contacts were located predominantly on basal dendrites and the synapses are reliable but of only relatively low efficacy ($1.0 \pm 0.7$ mV; see below). Sensory excitation arriving via L4 spiny stellate axons and in addition by direct thalamocortical afferents to lower layer 2/3 initiates feed-forward excitation between L2/3 pyramidal cells first within the PW column and then spreading also in the neighbouring, surround whisker (SuW) columns (Laaris *et al.* 2000; Brecht *et al.* 2003; Petersen *et al.* 2003). The 'innervation domain' of the L2/3-to-L2/3 connections in a column almost exactly overlaps with the innervation domain of the afferent L4-to-L2/3 connections in the same column (Lübke *et al.* 2003). The anatomical and functional parameters determining synaptic efficacy of the vertical afferents from layer 4 and of the horizontal afferents in layer 2/3 are quite comparable (Table 1).

The present results are relevant to the question of which factors govern the horizontal spread of excitation *within* the PW column and *out of* the PW into the SuW columns when a single whisker has been deflected. To resolve this one has to determine under which conditions the excitation arriving via the L4 afferents is transformed by the intralaminar network of layer 2/3 into AP firing thereby mediating the spread of excitation over the cortical surface.

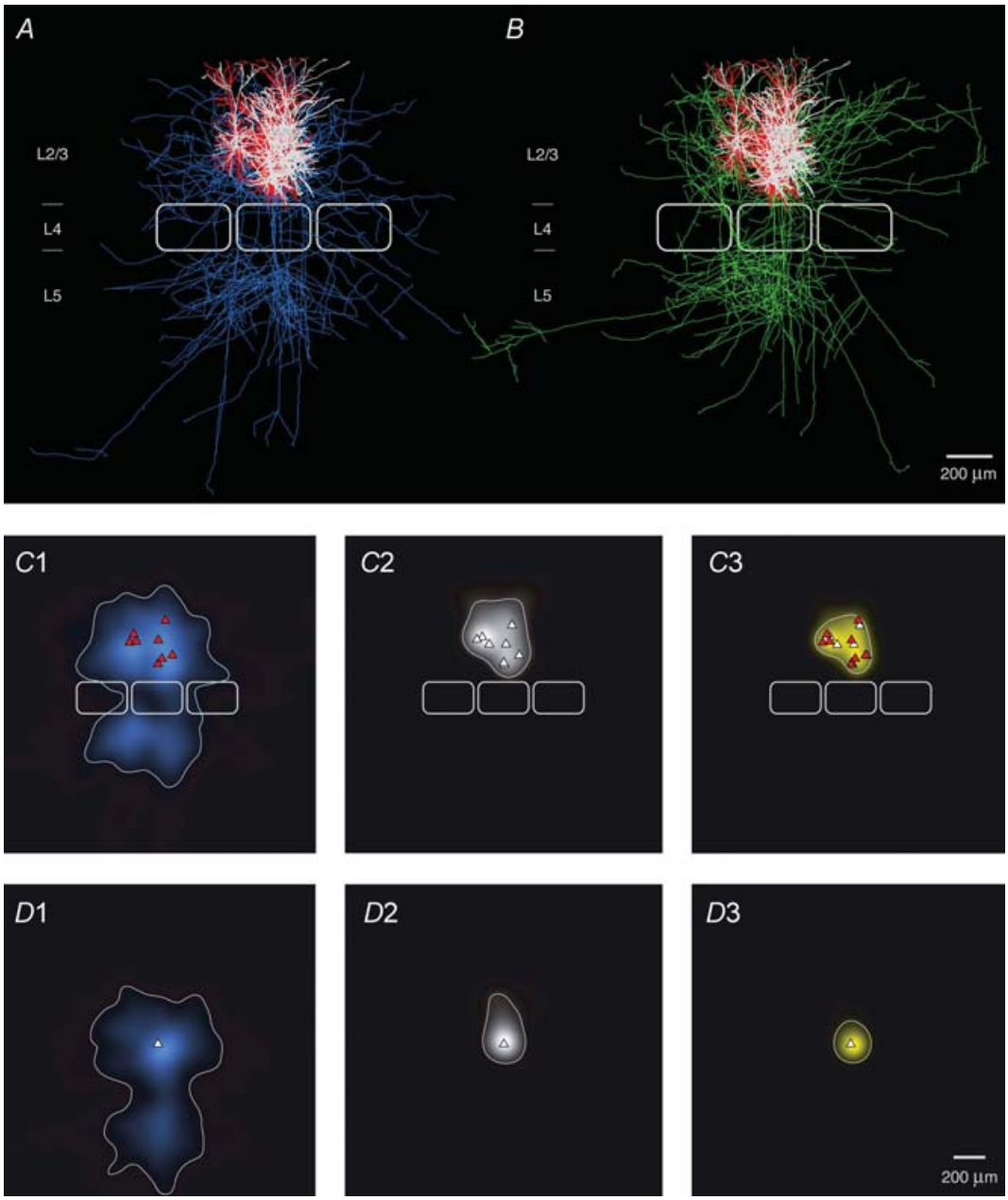


**Figure 7. Superposition of pairs of synaptically connected L2/3 pyramidal cells**
*A* and *B*, 2D computer-aided reconstructions of pairs of synaptically connected L2/3 pyramidal cells superimposed and aligned with respect to the barrel centre. The dendritic domains of the presynaptic pyramidal cell are shown in red (*A*), those of the postsynaptic pyramidal cells in white; presynaptic axons are in blue and postsynaptic axons in green. The central barrel has the average dimensions given in Table 2. The outlines of two neighbouring barrels were added symbolically for clarity. *C*, 2D maps of axonal (*C1*) and dendritic 'length density' (*C2*) of synaptically coupled pairs of L2/3 pyramidal cells, aligned with respect to the centre of the barrel. The predicted innervation domain (*C3*, yellow) of postsynaptic L2/3 dendrites by presynaptic L2/3 axons is given by the product of the presynaptic L2/3 axonal density and the postsynaptic L2/3 dendritic density. Contours (thin lines) enclosing 80% of the integrated density are shown superimposed. Positions of presynaptic L2/3 pyramidal cell somata (red triangles), postsynaptic L2/3 pyramidal cell somata (white triangles) and outlines of barrels (thick white lines) are indicated symbolically. *D*, 2D map of axonal (*D1*) and dendritic 'length density' (*D2*) centred on the location of the postsynaptic L2/3 pyramidal cell soma (white triangle) of each pair of reconstructions. For these maps the same eight L2/3 pyramidal cell pairs plus two additional pairs (for which the location with respect to the barrel was not recovered) were used. Note that mainly the basal dendritic field contributes to the innervation domain (*D3*, yellow).

### Local properties of L2/3 pyramidal cells

**Comparison with previous results.** Synaptic connections between pairs of L2/3 pyramidal cells have been studied in several cortical areas, most notably in the visual, auditory, somatosensory and motor cortex of juvenile and mature rats (Mason *et al.* 1991; Thomson & Deuchars, 1997; Thomson, 1997; Hardingham & Larkman, 1998; Thomson & Bannister, 1998; Egger *et al.* 1999; Reyes & Sakmann, 1999; Atzori *et al.* 2001; Thomson & West, 1993; Thomson *et al.* 2002; Holmgren *et al.* 2003; Koester & Johnston, 2005). The mean unitary EPSP amplitude from all these studies was about 0.8 mV (range 0.3–1.7 mV with no obvious differences between cortical areas), a value very close to that observed in the present study ($1.0 \pm 0.7$ mV). L2/3–L2/3 connections are generally reliable with c.v. values varying from 0.10 to 0.55, although not as reliable as those between L4 spiny neurones and L2/3 pyramidal cells. The failure rate for L2/3–L2/3 connections in the barrel cortex has been reported to be low (7%, Atzori *et al.* 2001; 22%, Koester & Johnston, 2005; compared to 3% observed in this study), suggesting a relatively high reliability. However, in auditory cortex L2/3 pyramidal cell connections have only either a low or an intermediate release probability, indicating area specific differences between L2/3–L2/3 connections (Atzori *et al.* 2001).

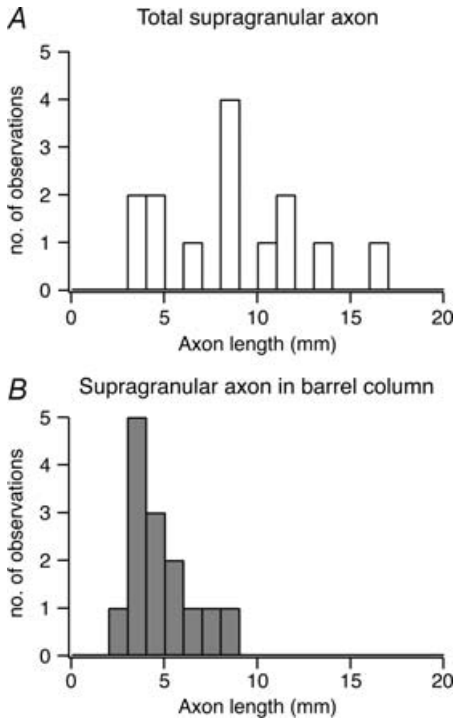


**Figure 8. Axonal length in supragranular layers**
*A*, histogram of the distribution of total axonal length of L2/3 pyramidal cells in the supragranular layer ($n = 14$ of 7 synaptic connections) and *B*, of the intracolumnar axonal length in the supragranular layer (i.e. the supragranular axon length within the home column). Only those synaptic connections were used for which the L2/3 pyramidal cell axon displayed no obvious truncation throughout layers 1–6. Note that the distribution of the total supragranular axon length is highly variable while that of the intracolumnar axon length is relatively narrow.

In an *in vivo* study (Crochet *et al.* 2005), synaptically connected L2/3 pyramidal cells have been shown to be in either a 'silent' or an 'active' state. In the 'silent' state, the mean EPSP amplitude is 0.7 mV with a c.v. of 0.45 while in the 'active' state it decreases to 0.5 mV and is much less reliable (c.v. = 1.57). The EPSP amplitudes in the silent state are roughly similar to those measured here ($1.0 \pm 0.7$ mV), despite the authors' assumption that *in vivo* the free extracellular $Ca^{2+}$ concentration (and therefore the release probability) is lower than that in slice ASCF; this indicates that the slice situation is probably similar to the 'silent' or 'down' state of neurones (Petersen *et al.* 2003).

So far, L2/3 pyramidal cells have not been classified into morphologically distinct subgroups. While Larkman & Mason (1990) reported superficial L2/3 pyramidal cells with short apical dendrites and deeper neurones with longer apical dendrites, they did not quantify the relationship between the length of the apical dendrite and the extent of the apical tuft. As superficial pyramidal cells have broader and more elaborate tuft regions, inputs from the paralemniscal thalamic afferents as well as from L5A pyramidal cells could be integrated over a larger cortical area (Feldmeyer *et al.* 2005; Shepherd & Svoboda, 2005; Shepherd *et al.* 2005). This might result in different RF properties for deep and superficial pyramidal cells in layer 2/3, which should be examined by *in vivo* studies.

**Synaptic efficacy.** The size of the unitary EPSP evoked by a single presynaptic AP is given by $\Delta V = n_b q_S p_r$ with $n_b$, $q_S$ and $p_r$ as defined above. The unitary EPSP in L2/3-to-L2/3 connections is on average around 1 mV, which is larger than that of unitary EPSPs at the L4-to-L2/3 connections (0.7 mV; Feldmeyer *et al.* 2002). In pairs with morphologically identified synaptic contacts, the mean EPSP amplitude was almost identical (0.5 mV and 0.4 mV for L4–L2/3 and L2/3–L2/3 connections, respectively) with the number of contacts being 4.5 and their mean distance from the soma being 69 $\mu$m for L4–L2/3 connections and 2.8 contacts and a mean distance of 97 $\mu$m for L2/3–L2/3 connections (the value of 55 $\mu$m reported by Koester & Johnston (2005) is likely to be an underestimate as this study was biased towards contacts close to the soma. The release probability for individual contacts has been estimated to

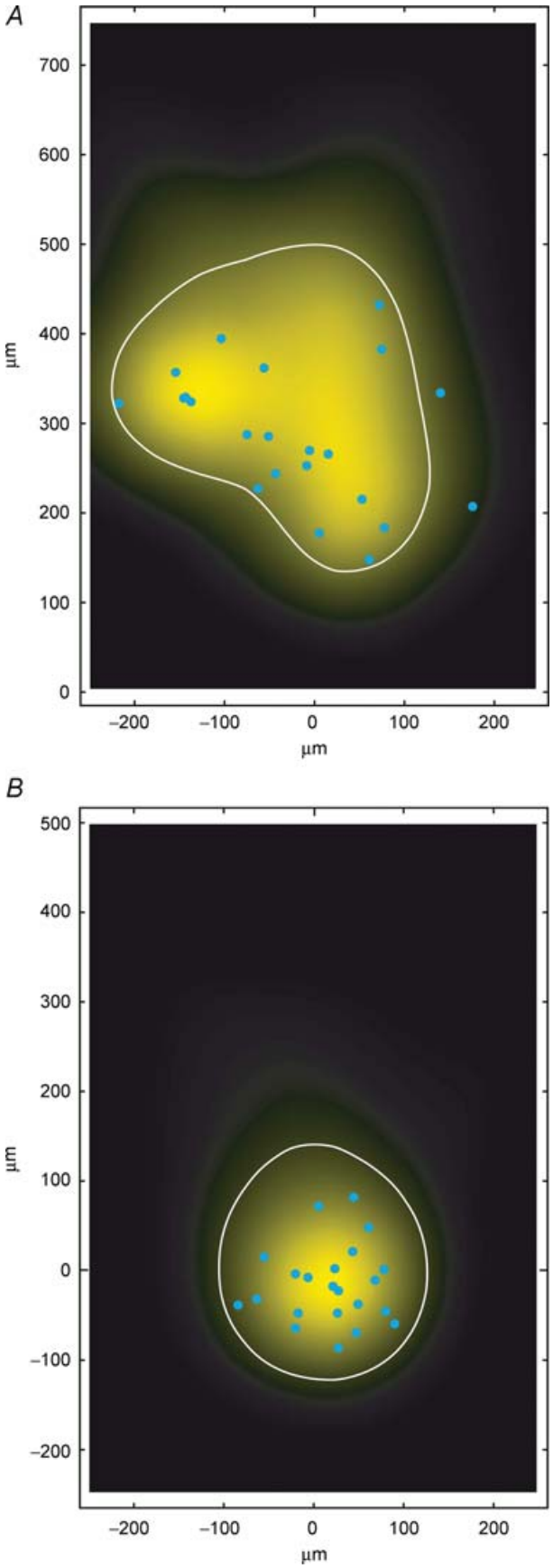


be 0.79 at the L4–L2/3 (Silver *et al.* 2003) and 0.46 at the L2/3–L2/3 connection in somatosensory cortex (Koester & Johnston, 2005), respectively. Since both the number and the geometric distance of contacts are not vastly different for the two connection types, this may suggest that the quantal EPSP amplitude $q_S$ for the L2/3–L2/3 connection is on average somewhat larger than at the L4–L2/3 connection.

### Architecture of inputs to L2/3 pyramidal cells

*In vivo* whole cell recordings from barrel-related pyramidal cells in layer 2/3 have indicated that L2/3 pyramidal cells have broad *sub*threshold RFs, but narrow *supra*threshold RFs (Moore & Nelson, 1998; Margrie *et al.* 2002; Brecht *et al.* 2003). The subthreshold RFs reflect the structure of the network of synaptic inputs to L2/3 pyramidal cells. Importantly, these RFs are dynamic as they expand rapidly 20–30 ms after stimulus onset before collapsing during the following 100–200 ms (Brecht *et al.* 2003).

The barrel-related L2/3 pyramidal cells are elements of the supragranular network that receives direct input from the thalamus (VPM), the deeper layers L4 and L5A as well as horizontal input from within layer 2/3 (Fig. 10; Feldmeyer *et al.* 1999, 2005; Shepherd & Svoboda, 2005; Shepherd *et al.* 2005); some input from L5B pyramidal cells may exist as well (Thomson & Bannister, 1998). The degree of excitation of L2/3 pyramidal cells, as measured by subthreshold RFs, thus depends *firstly* on the anatomical convergence of the axonal arbours projecting from these neurones into layer 2/3, *secondly* on the efficacy of these connections in eliciting APs in their target L2/3 pyramidal cells, and *thirdly* on the synchrony of synaptic inputs of a particular type of projection. Together the time dependent PSP and AP patterns in layer 2/3 'represent' a sensory stimulus as a cortical 'map'. The results of the present experiments relevant for constructing such a map are the contours of the innervation domains of L4 and L2/3 afferents (Fig. 10), the size of unitary EPSPs of

**Figure 9. Innervation domain of presynaptic L2/3 axons on postsynaptic L2/3 pyramidal cell dendrites**
*A*, close-up of the predicted innervation domain of postsynaptic L2/3 pyramidal cell dendrites by presynaptic L2/3 axons, aligned to the barrel centre (same data as in Fig. 7*C3*, i.e. $n = 8$, number of contacts = 22). A contour (white line) enclosing 80% of the integrated density and the locations of light microscopically identified synaptic contacts (blue circles) of eight L2/3 pyramidal cell pairs (blue cicles, $n = 22$) are superimposed. *B*, predicted innervation domain centred on the location of the postsynaptic L2/3 pyramidal cell somata (same data as for Fig. 7*D3*). Note that both the predicted innervation domain and the distribution of light microscopically identified synaptic contacts (blue circles) are much more compact in this representation, being confined mostly to the basal dendrites of the L2/3 pyramidal cells. All contacts were located within the contour (thin lines) enclosing 80% of the integrated density.

L2/3-to-L2/3 connections and the relative independence of unitary EPSP amplitudes on the distance between synaptically connected neurones (at least within the innervation domain; but see Holmgren *et al.* 2003).

To estimate the synaptic input to a L2/3 pyramidal cell from the columnar L2/3-to-L2/3 connections one assumes that L4-to-L2/3 feed-forward input (Lübke *et al.* 2003) generates an initial pattern of APs in layer 2/3. These APs then by L2/3-to-L2/3 connections generate additional, late excitation in the PW column. The additional L2/3-to-L2/3 excitation is delayed by several milliseconds or even tens of milliseconds with respect to the L4-to-L2/3 input. The later depolarization depends on the anatomical convergence as well as the synaptic efficacy of L2/3-to- L2/3 connections.

**Anatomical convergence: estimate of L2/3 pyramidal cells targeting a L2/3 pyramidal cell in a column.** A rough estimate of the number of L2/3 pyramidal cells that innervate a L2/3 pyramidal cell in the same PW column can be derived from the number of synaptic boutons of the pyramidal cell axon that is located within the 'innervation-domain' of the column. The mean number of 0.3 boutons per micrometre axon length, and an axonal length of 2881 $\mu$m yields a total number of ~900 boutons in the (barrel-centred) innervation domain of each pyramidal cell. When the number of boutons in the innervation domain is divided by the average number of synaptic contacts made in a L2/3-to-L2/3 pyramidal cell pair (~3 contacts established per connection assuming a single release site per contact: Silver *et al.* 2003; Biro *et al.* 2005), a single L2/3 pyramidal cell should innervate about 300 postsynaptic neurones. Assuming that a 10% fraction of the boutons establishes synaptic contacts on inhibitory interneurones (numbers vary between 5% and 25%; see, e.g. DeFelipe & Farinas, 1992; Beaulieu, 1993; DeFelipe *et al.* 1999; see also Supplemental Online Material; Supplemental Fig. 4), the number of L2/3 pyramidal cells targeted by a single L2/3 pyramidal cell is probably in the order of 270 barrel-related pyramidal cells. For symmetry reasons, this is also the number of L2/3 pyramidal cells in a column by which a single L2/3 pyramidal cell is innervated, i.e. that converge on a single pyramidal cell. Thus, the numbers of barrel-related L2/3 pyramidal cells and L4 spiny neurones innervating a single L2/3 pyramidal cell is comparable (300–400, Lübke *et al.* 2003 *versus* 270, this report). This estimate differs significantly from that of Holmgren *et al.* (2003) who calculated about 60 inputs within a distance of $\pm$200 $\mu$m, a region about the size of the innervation domain. In part this may be due to the larger mean distance between synaptically coupled neurones in their study, but even for short distances between somata

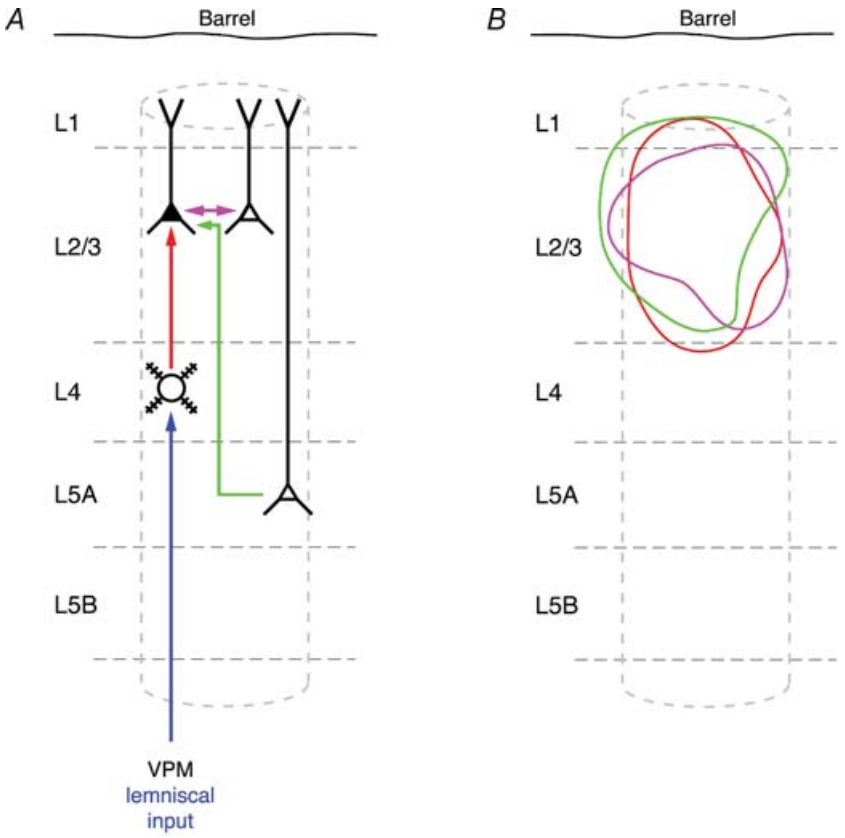


**Figure 10. Schematic representation of L2/3 dendrites innervated by different cortical projections**
*A*, schematic barrel column showing intracortical synaptic connections as well as input from the lemniscal thalamic nucleus (ventroposterior medial nucleus; VPM). The different synaptic connections are colour coded: intracortical connections are in red, violet and green; the thalamocortical inputs are drawn in dark blue (from VPM) *B*, innervation domains (80% contour lines) for the three types of excitatory synaptic connections in which L2/3 pyramidal cells are the postsynaptic (target) neurones (L4–L2/3 connection, red; L2/3–L2/3 connection, violet; L5A–L2/3 connection, green). Data for L4–L2/3 connections are taken from Lübke *et al.* (2003). Prospective L5A–L2/3 innervation domains were constructed using the dendritic domain of L2/3 pyramidal cells from Lübke *et al.* (2003) and this study and the axonal domain of L5A pyramidal cells from Feldmeyer *et al.* (2005). Note that the innervation domains show considerable overlap within the cortical column.

($< 25\ \mu$m) the connectivity estimates were low compared to this and other studies (Mason *et al.* 1991; Hardingham & Larkman, 1998; Atzori *et al.* 2001; Thomson *et al.* 2002). Furthermore, it is unlikely that 60 inputs can sustain AP firing in the L2/3 network given the sparse AP activity reported from *in vivo* studies (Brecht *et al.* 2003).

**Functional convergence: estimate of active L2/3 pyramidal cell inputs.** One can roughly estimate the amplitude of the late compound EPSP in a L2/3 pyramidal cell following deflection of the PW. The late EPSP is evoked by the columnar L2/3-to-L2/3 circuit after the L4-to-L2/3 input has generated early compound EPSPs and an initial spatially distributed train of APs in layer 2/3. We assume that each pyramidal cell in layer 2/3 is innervated by 270 other barrel-related pyramidal cells. As a lower estimate, 3% of these pyramidal cells generate an AP upon deflection of a single whisker (Brecht *et al.* 2003). Hence, each L2/3 pyramidal cell in the PW-column would receive about eight additional unitary synaptic inputs (because 3% of the 270 anatomical inputs are active) from other pyramidal cells located in the L2/3 network of the same column. Since a single L2/3 input generates a unitary EPSP size of about 1 mV, the maximal peak of the late compound EPSP is ∼8 mV. Because of the jitter of APs in layer 2/3 the late depolarization is, however, much smaller. If the single cell response probability for L2/3 pyramidal cells is 0.11, i.e. ∼10% (upper estimate; C.P.J. de Kock & B. Sakmann, unpublished observation), the late compound EPSP could be substantially higher. Thus, the L2/3-to-L2/3 connections could amplify the excitation evoked by feed-forward excitatory input from layer 4 (Douglas & Martin, 2004).

## Vertical excitatory projections of L2/3 pyramidal cells in infragranular layers

Anatomical reconstructions of connected cell pairs (Feldmeyer *et al.* 2002; Lübke *et al.* 2003) indicate that L2/3 axonal arbours spread laterally across PW column borders also in infragranular layers 5 and 6. These are collaterals, which branch off from the vertically orientated main axon of the L2/3 pyramidal cells. The main axons project vertically to the subcortical white matter and give rise to axon bundles projecting to the contralateral hemisphere, to S2 and to the motor cortex (Hoffer *et al.* 2003, 2005). The infragranular projection tangential to the pial surface of L2/3 pyramidal cells is most dense in layer 5A. The overlap between L2/3 axonal arbours and L5A dendritic arbours is forming an innervation domain with the highest density of potential L2/3-to-L5A synaptic contacts underneath a barrel wall. Presumably it is part of an excitatory cortical feedback loop connecting reciprocally layer 2/3 and 5A (Feldmeyer *et al.* 2005; Shepherd & Svoboda, 2005; Schubert *et al.* 2006).

## Conclusions

The major aim of the present study in conjunction with our previous work on the anatomical and functional connectivity of different classes of neurones in the barrel cortex is to delineate how a simple sensory stimulus, a brief whisker deflection, is encoded by PSPs and APs in L2/3 and to quantify the anatomical and functional determinants of the respective representational maps.

Figure 11 illustrates schematically part of a pattern of feed-forward vertical input combined with intralaminar

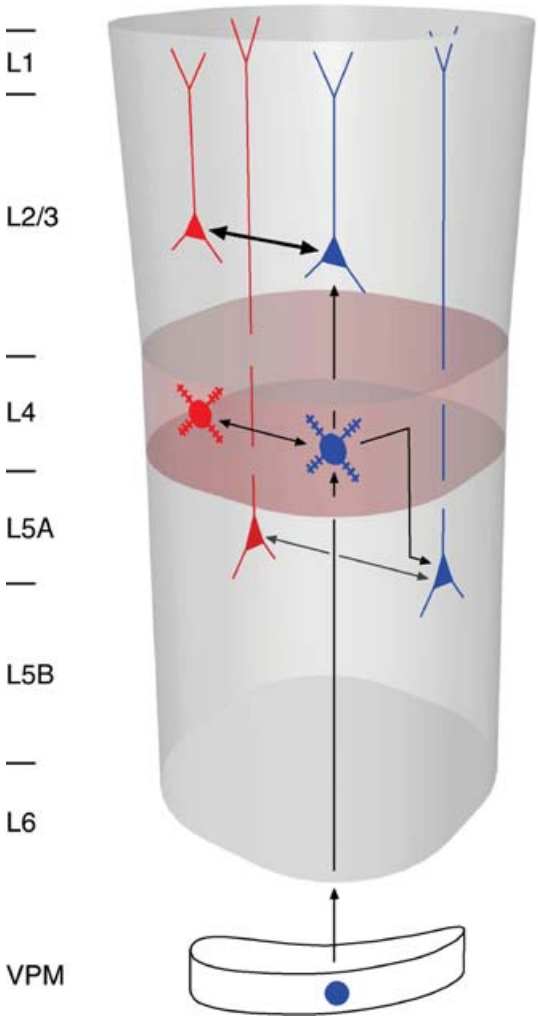


**Figure 11. Schematic view of L2/3-to-L2/3 feedback connections in a cortical column**
In each of the cortical layers (layer 2/3, 4 and 5A) pyramidal cells receive vertical interlaminar feed-forward input (blue cell symbols; vertical arrows) and intralaminar feedback excitation (horizontal arrows). In each layer the intralaminar connections (L2/3–L2/3, L4–L4 and L5A–L5A) could amplify vertical input. For emphasis, the arrow representing the L2/3-L2/3 connection is given in bold.

(reciprocal) feedback excitation examined so far by paired recordings in layers 4, 2/3, 5A and 5B (Markram *et al.* 1997; Feldmeyer *et al.* 1999, 2002, 2005; Bruno & Sakmann, 2006). Here vertical thalamic input from VPM excites spiny cells in layer 4 which excite other cells within layer 4 to generate early APs. Via the intralaminar reciprocal excitatory connections the AP activity will be amplified provided the early APs are synchronous. A similar pattern of vertical feed-forward and horizontal feed-back excitation applies to layer 2/3 and 5A. Both are excited by feed-forward input from layer 4 that can be amplified by the intralaminar feed-back excitation. Surprisingly, all L2/3 pyramidal cells in the principal column respond, upon a single PW whisker deflection, with an early compound EPSP (Brecht *et al.* 2003). These early EPSPs reflect the high divergence of L4-to-L2/3 connections. The later compound EPSPs reflect the high divergence of connections between L2/3 pyramidal cells. Functionally both L4-to-L2/3 and L2/3-to-L2/3 connections are of high reliability but of relatively low efficacy. APs generated by these two connections signal to virtually every barrel-related cell in layer 2/3 the deflection of a whisker. In other words, the *input* to (and subthreshold excitation within) layer 2/3 is 'dense'. However, only a small fraction, 3–11%, of L2/3 pyramidal cells respond with APs, and thus the *output* from layer 2/3 to other cortical areas like S2 or M1 is 'sparse'. This pattern of *dense coding* at the input to a layer (meaning that in a large fraction of cells in a layer, PSPs are generated reliably) and *sparse output* from a layer (meaning in a small fraction of neurones APs are generated) is seen in layers 4, 2/3 and layer 5. The intralaminar feed-forward connections observed in each layer could in certain circumstances selectively amplify excitation in a particular layer and thus enhance its output to the specific target cells.

## References


Agmon A & Connors BW (1991). Thalamocortical responses of mouse somatosensory (barrel) cortex in vitro. *Neurosci* **41**, 365–379.

Armstrong-James M (1995). The nature and plasticity of sensory processing within adult rat barrel cortex. In *The Barrel Cortex of Rodents*, ed. Jones EG & Diamond IT, pp. 333–374. Plenum Press, New York.

Armstrong-James M, Callahan CA & Friedman MA (1991). Thalamo-cortical processing of vibrissal information in the rat. I. Intracortical origins of surround but not centre-receptive fields of layer IV neurones in the rat S1 barrel field cortex. *J Comp Neurol* **303**, 193–210.

Armstrong-James M & Fox K (1987). Spatiotemporal convergence and divergence in the rat S1 'barrel' cortex. *J Comp Neurol* **263**, 265–281.

Armstrong-James M, Fox K & Das-Gupta A (1992). Flow of excitation within rat barrel cortex on striking a single vibrissa. *J Neurophysiol* **68**, 1345–1358.

Atzori M, Lei S, Evans DI, Kanold PO, Phillips-Tansey E, McIntyre O & McBain CJ (2001). Differential synaptic processing separates stationary from transient inputs to the auditory cortex. *Nat Neurosci* **4**, 1230–1237.

Beaulieu C (1993). Numerical data on neocortical neurons in adult rat, with special reference to the GABA population. *Brain Res* **609**, 284–292.

Biro AA, Holderith NB & Nusser Z (2005). Quantal size is independent of the release probability at hippocampal excitatory synapses. *J Neurosci* **25**, 223–232.

Brecht M, Roth A & Sakmann B (2003). Dynamic receptive fields of reconstructed pyramidal cells in layers 3 and 2 of rat somatosensory barrel cortex. *J Physiol* **553**, 243–265.

Brecht M & Sakmann B (2002). Dynamic representation of whisker deflection by synaptic potentials in spiny stellate and pyramidal cells in the barrels and septa of layer 4 rat somatosensory cortex. *J Physiol* **543**, 49–70.

Bruno RM & Sakmann B (2006). Cortex is driven by weak but synchronously active thalamocortical synapses. *Science* **312**, 1622–1627.

Crochet S, Chauvette S, Boucetta S & Timofeev I (2005). Modulation of synaptic transmission in neocortex by network activities. *Eur J Neurosci* **21**, 1030–1044.

DeFelipe J & Farinas I (1992). The pyramidal neuron of the cerebral cortex: morphological and chemical characteristics of the synaptic inputs. *Prog Neurobiol* **39**, 563–607.

DeFelipe J, Marco P, Busturia I & Merchan-Perez A (1999). Estimation of the number of synapses in the cerebral cortex: methodological considerations. *Cereb Cort* **9**, 722–732.

Douglas RJ & Martin KA (2004). Neuronal circuits of the neocortex. *Annu Rev Neurosci* **27**, 419–451.

Egger V, Feldmeyer D & Sakmann B (1999). Coincidence detection and efficacy changes in synaptic connections between spiny stellate neurons of the rat barrel cortex. *Nat Neurosci* **2**, 1098–1105.

Feldmeyer D, Egger V, Lübke J & Sakmann B (1999). Reliable synaptic connections between pairs of excitatory layer 4 neurones within a single 'barrel' of developing rat somatosensory cortex. *J Physiol* **521**, 169–190.

Feldmeyer D, Lübke J, Silver RA & Sakmann B (2002). Synaptic connections between layer 4 spiny neurone–layer 2/3 pyramidal cell pairs in juvenile rat barrel cortex: physiology and anatomy of interlaminar signalling within a cortical column. *J Physiol* **538**, 803–822.

Feldmeyer D, Roth A & Sakmann B (2005). Monosynaptic connections between pairs of spiny stellate cells in layer 4 and pyramidal cells in layer 5A indicate that lemniscal and paralemniscal afferent pathways converge in the infragranular somatosensory cortex. *J Neurosci* **25**, 3423–3431.

Feldmeyer D & Sakmann B (2000). Synaptic efficacy and reliability of excitatory connections between the principal neurones of the input (layer 4) and output layer (layer 5) of the neocortex. *J Physiol* **525**, 31–39.

Fox K, Wright N, Wallace H & Glazewski S (2003). The origin of cortical surround receptive fields studied in the barrel cortex. *J Neurosci* **23**, 8380–8391.

Goldreich D, Kyriazi HT & Simons DJ (1999). Functional independence of layer IV barrels in rodent somatosensory cortex. *J Neurophysiol* **82**, 1311–1316.

Gottlieb JP & Keller A (1997). Intrinsic circuitry and physiological properties of pyramidal neurons in rat barrel cortex. *Exp Brain Res* **115**, 47–60.

Hardingham NR & Larkman AU (1998). The reliability of excitatory synaptic transmission in slices of rat visual cortex in vitro is temperature dependent. *J Physiol* **507**, 249–256.

Hoffer ZS, Arantes HB, Roth RL & Alloway KD (2005). Functional circuits mediating sensorimotor integration: quantitative comparisons of projections from rodent barrel cortex to primary motor cortex, neostriatum, superior colliculus, and the pons. *J Comp Neurol* **488**, 82–100.

Hoffer ZS, Hoover JE & Alloway KD (2003). Sensorimotor corticocortical projections from rat barrel cortex have an anisotropic organization that facilitates integration of inputs from whiskers in the same row. *J Comp Neurol* **466**, 525–544.

Holmgren C, Harkany T, Svennenfors B & Zilberter Y (2003). Pyramidal cell communication within local networks in layer 2/3 of rat neocortex. *J Physiol* **551**, 139–153.

Kleinfeld D & Delaney KR (1996). Distributed representation of vibrissa movement in the upper layers of somatosensory cortex revealed with voltage-sensitive dyes. *J Comp Neurol* **375**, 89–108.

Koester HJ & Johnston D (2005). Target cell-dependent normalization of transmitter release at neocortical synapses. *Science* **308**, 863–866.

Kwegyir-Afful EE, Bruno RM, Simons DJ & Keller A (2005). The role of thalamic inputs in surround receptive fields of barrel neurons. *J Neurosci* **25**, 5926–5934.

Laaris N, Carlso GC & Keller A (2000). Thalamic-evoked synaptic interactions in barrel cortex revealed by optical imaging. *J Neurosci* **20**, 1529–1537.

Larkman A & Mason A (1990). Correlations between morphology and electrophysiology of pyramidal neurons in slices of rat visual cortex. I. Establishment of cell classes. *J Neurosci* **10**, 1407–1414.

Lübke J, Egger V, Sakmann B & Feldmeyer D (2000). Columnar organization of dendrites and axons of single and synaptically coupled excitatory spiny neurons in layer 4 of the rat barrel cortex. *J Neurosci* **20**, 5300–5311.

Lübke J, Roth A, Feldmeyer D & Sakmann B (2003). Morphometric analysis of the columnar innervation domain of neurons connecting layer 4 and layer 2/3 of juvenile rat barrel cortex. *Cereb Cort* **13**, 1051–1063.

Margrie TW, Brecht M & Sakmann B (2002). In vivo, low-resistance, whole-cell recordings from neurons in the anaesthetized and awake mammalian brain. *Pflugers Arch* **444**, 491–498.

Markram H, Lübke J, Frotscher M, Roth A & Sakmann B (1997). Physiology and anatomy of synaptic connections between thick tufted pyramidal neurons in the developing rat neocortex. *J Physiol* **500**, 409–440.

Mason A, Nicoll A & Stratford K (1991). Synaptic transmission between individual pyramidal neurons of the rat visual cortex *in vitro*. *J Neurosci* **11**, 72–84.

Moore CI & Nelson SB (1998). Spatio-temporal subthreshold receptive fields in the vibrissa representation of rat primary somatosensory cortex. *J Neurophysiol* **80**, 2882–2892.

Petersen CCH, Hahn TT, Mehta M, Grinvald A & Sakmann B (2003). Interaction of sensory responses with spontaneous depolarization in layer 2/3 barrel cortex. *Proc Natl Acad Sci U S A* **100**, 13638–13643.

Reyes A & Sakmann B (1999). Developmental switch in the short-term modification of unitary EPSPs evoked in layer 2/3 and layer 5 pyramidal neurons of rat neocortex. *J Neurosci* **19**, 3827–3835.

Schubert D, Kötter R, Luhmann HJ & Staiger JF (2006). Morphology, electrophysiology and functional input connectivity of pyramidal neurons characterizes a genuine layer via in the primary somatosensory cortex. *Cereb Cort* **16**, 223–236.

Shepherd GMG, Stepanyants A, Bureau I, Chklovskii D & Svoboda K (2005). Geometric and functional organization of cortical circuits. *Nat Neurosci* **8**, 782–790.

Shepherd GMG & Svoboda K (2005). Laminar and columnar organization of ascending excitatory projections to layer 2/3 pyramidal neurons in rat barrel cortex. *J Neurosci* **25**, 5670–5679.

Silver RA, Lübke J, Sakmann B & Feldmeyer D (2003). High-probability uniquantal transmission at excitatory synapses in barrel cortex. *Science* **302**, 1981–1984.

Simons DJ (1978). Response properties of vibrissa units in rat SI somatosensory neocortex. *J Neurophysiol* **41**, 798–820.

Simons DJ (1995). Neuronal integration in the somatosensory whisker/barrel cortex. In *The Barrel Cortex of Rodents*, ed.Jones EG & Diamond IT, pp. 262–298. Plenum Press, New York.

Simons DJ & Carvell GE (1989). Thalamocortical response transformation in the rat vibrissa/barrel system. *J Neurophysiol* **61**, 311–330.

Stratford KJ, Tarczy-Hornoch K, Martin KAC, Bannister NJ & Jack JJB (1996). Excitatory synaptic inputs to spiny stellate cells in cat visual cortex. *Nature* **382**, 258–261.

Thomson AM (1997). Activity-dependent properties of synaptic transmission at two classes of connections made by rat neocortical pyramidal axons *in vitro*. *J Physiol* **502**, 131–147.

Thomson AM & Bannister AP (1998). Postsynaptic target selection by descending layer III pyramidal cell axons: Dual intracellular recordings and biocytin filling in slices of rat neocortex. *Neurosci* **84**, 669–683.

Thomson AM, Bannister AP, Mercer A & Morris OT (2002). Target and temporal pattern selection at neocortical synapses. *Phil Trans Roy Soc Lond B Biol Sci* **357**, 1781–1791.

Thomson AM & Deuchars J (1997). Synaptic interactions in neocortical local circuits: dual intracellular recordings in vitro. *Cereb Cort* **7**, 510–522.

Thomson AM & West DC (1993). Fluctuations in pyramid-pyramid excitatory postsynaptic potentials modified by presynaptic firing pattern and postsynaptic membrane potential using paired intracellular recordings in rat neocortex. *Neurosci* **54**, 329–346.

Timofeeva E, Lavallee P, Arsenault D & Deschênes M (2004). Synthesis of multiwhisker-receptive fields in subcortical stations of the vibrissa system. *J Neurophysiol* **9**, 1510–1515.

Woolsey TA & van der Loos H (1970). The structural organization of layer IV in the somatosensory region (SI) of mouse cerebral cortex. *Brain Res* **17**, 1970.

## Acknowledgements

We would like to thank Dr Arnd Roth for his kind help with the density plots and Sigrun Nestel, Barbara Joch and Marlies Kaiser for excellent technical support. We would also like to thank Drs Arnd Roth, Randy Bruno and Gabriele Radnikow for their helpful comments on manuscript. This work was supported by the Max-Planck Society, the Helmholtz Society, a grant from the BMBF (to J.L.) and a grant from the Volkswagenstiftung (to D.F.).

## Supplemental material

The online version of this paper can be accessed at:
DOI: 10.1113/jphysiol.2006.105106
http://jp.physoc.org/cgi/content/full/jphysiol.2006.105106/DC1

and contains supplemental material consisting of four figures, as follows.

Supplemental Figure 1. IR-DIC images of synaptically connected L2/3 pyramidal cells and relationship between soma distance and EPSP amplitude

Supplemental Figure 2. Time course and amplitude of EPSPs in an individual L2/3 pyramidal cell pair

Supplemental Figure 3. EPSCs time course at the L2/3-L2/3 pyramidal cell connection

Supplemental Figure 4. Target structures of L2/3 pyramidal cell axons

This material can also be found as part of the full-text HTML version available from http://www.blackwell-synergy.com